Helicity-dependent reaction $\vec{\gamma}\vec{d} \to \pi NN$ and its contribution to the GDH sum rule for the deuteron

M. I. Levchuk*
B.I. Stepanov Institute of Physics, 220072 Minsk, Belarus
(Dated: November 10, 2010)

Helicity-dependent incoherent pion photoproduction in the reaction $\vec{\gamma}\vec{d} \to \pi NN$ is studied in the framework of the diagrammatic approach. Contributions to the reaction amplitude from diagrams corresponding to impulse approximation as well as NN and πN interactions in the final state have been evaluated. The elementary $\gamma N \to \pi N$ operator is taken from the MAID and SAID models. A detailed comparison of the predictions with recent experimental data by the GDH and A2 collaborations at energies below 500 MeV is presented. Reasonable agreement with the data on the yields and cross sections for polarized beam and polarized target has been achieved in all channels. The unpolarized data of the GDH and A2 collaborations have also been analyzed within the approach. A strong overestimation for the neutral channel has been found. At the same time, the model provides a quite satisfactory description of the unpolarized data for the charged channels. The sensitivity of the obtained results to the choice of the elementary $\gamma N \to \pi N$ operator is discussed in detail. The contribution of the $\gamma d \to \pi NN$ reaction to the GDH sum rule for the deuteron up to a photon energy of 1.65 GeV has been evaluated with the result of 235 ± 25 μb.

PACS numbers: 13.60.Le, 21.45.Bc, 25.20.Lj

I. INTRODUCTION

For more than a decade, the GDH and A2 collaborations have been carrying out intense experimental studies aimed at the verification of the famous Gerasimov-Drell-Hearn (GDH) sum rule [1, 2]. A comprehensive overview concerning the status of these experiments is given in Ref. [3].

The GDH sum rule gives an integral relation between anomalous magnetic moment κ of a spin-S particle and the difference of the total photoabsorption cross sections with parallel, σ_P, and antiparallel, σ_A, photon and target spin alignments and reads

$$\frac{4\pi^2\alpha\kappa^2}{m^2}\, S = \int_0^\infty \frac{\sigma_P(E_\gamma) - \sigma_A(E_\gamma)}{E_\gamma}\, dE_\gamma, \tag{1}$$

where E_γ is the photon laboratory energy, m is the particle mass, and $\alpha = 1/137$. Equation (1) shows that ground-state properties given by κ and m are related to the energy-weighted excitation spectrum of the particle. The GDH sum rule relies on the basic physics principles of Lorenz and gauge invariance, unitarity, crossing symmetry, and an unsubtracted dispersion relation applied to the forward Compton amplitude. Therefore, measurements of the right-hand side (rhs) of this equation can serve as a fundamental cross-check of these principles.

The left-hand side (lhs) of Eq. (1) for the proton is 205 μb. The integrand in the rhs of Eq. (1) at energies from 0.2 to 2.9 GeV was determined by the GDH and A2 collaborations in a series of experiments with circularly polarized photons and longitudinally polarized protons [4–6]. Involving theoretical predictions from threshold to 0.2 GeV and above 2.9 GeV, the GDH group obtained for the rhs of Eq. (1) $212 \pm 6(\text{stat}) \pm 16(\text{syst})$ μb, which is in good agreement with the GDH sum rule prediction.

The check of the isospin structure of the GDH sum rule requires measurements on the neutron. However, because of the absence of a stable, dense, free-neutron target, direct measurements for the neutron are impossible so that information on the neutron can be extracted from deuteron data. Experiments with circularly polarized photons and longitudinally polarized deuterons were also performed by the GDH and A2 collaborations [7–11] as well as by the LEGS Collaboration [12]. In fact, however, a contribution to the neutron GDH integral from deuteron data was extracted only in Ref. [8] and therewith in the limited energy range of 815–1825 MeV. The extraction procedure relied mainly on an assumption that at these energies the incoherent, quasi-free meson production reactions dominate; i.e. if one supposes that the equality $\Delta\sigma_d = \Delta\sigma_p + \Delta\sigma_n$ ($\Delta\sigma = \sigma_P - \sigma_A$) is valid. Such an assumption seems to be in general

*Electronic address: levchuk@dragon.bas-net.by

agreement with the results obtained by Arenhövel, Fix, and Schwamb (AFS) [13]. Using theoretical predictions for the unmeasured energy regions, the authors of Ref. [8] obtained the value of 226 μb for the rhs of Eq. (1) which is in agreement with the GDH sum rule value of 233 μb. Of course, this agreement should not be considered as an experimental verification of the GDH sum rule for the neutron, because the net experimental contribution to this value is only about 15%.

The helicity-dependent cross section on the deuteron in the energy range $200 < E_\gamma < 800$ MeV was also measured in Ref. [10]. Combining the obtained data with those from Ref. [8] and using again the assumption on the incoherency of the proton and neutron contributions in the range $200 < E_\gamma < 1800$ MeV, the authors of Ref. [10] obtained the value of 197 μb in this range. The said assumption seems to be rather rough below, say, 500 MeV, where the $\gamma d \to np$ and the $\gamma d \to \pi^0 d$ reactions contribute to the polarized total cross section, nevertheless, the extracted value indicates that the GDH integrals for the proton and neutron are of the same order of magnitude.

Together with the verification of the GDH sum rule for the neutron, the helicity-dependent cross sections on the deuteron are also required to test this sum rule for the deuteron itself. The anomalous magnetic moment of the deuteron is very small ($\kappa_d = -0.143$ nm) because, first, the anomalous magnetic moments of the proton and neutron are almost equal in magnitude but opposite in sign and, second, nucleon spins in the deuteron are predominantly parallel. In view of this, the lhs of Eq. (1) for the deuteron is 0.65 μb, which is more than two orders smaller than the nucleon values. Therefore, there should be large negative contributions almost totally canceling the nucleon contribution. This point was discussed for the first time in Ref. [14]. It was found that a huge negative contribution amounting to about -400 μb indeed exists and stems from the deuteron photodisintegration reaction. Later on, a comprehensive analysis of different channels in the deuteron GDH integral was performed within the AFS framework [13]. They evaluated effects from deuteron photodisintegration and single and double-pion production as well as from single-η production with the total result of 27.31 μb.

If one intends to extract the neutron value for the GDH integral from deuteron data or verify the deuteron GDH sum rule, in either case one has to be confident that theoretical models used in analyses of these data provide reliable descriptions of the helicity-dependent cross sections for different reactions on the deuteron. As was found in Refs. [13–15], a large contribution to the deuteron GDH integral stems from incoherent single-pion production $\gamma d \to \pi NN$.

Intense experimental investigations of the reaction $\vec{\gamma}\vec{d} \to \pi NN$ have recently been performed by the GDH and A2 collaborations [9–11]. References [9, 10] have provided data on the helicity-dependent total inclusive and semiexclusive cross sections in the energy range from 200 to 800 MeV. In the very recent work of the same collaborations [11], the helicity dependence of the differential cross section in the $\vec{\gamma}\vec{d} \to \pi NN$ channel has been measured for the first time in the Δ region. There are also measurements of the helicity-dependent total cross section of the reaction $\vec{\gamma}\vec{d} \to \pi^0 X$ [7, 12], where $X = np$ (the incoherent channel) or $X = d$ (the coherent channel).

The main goal of the present work is to analyze the data of Refs. [9–11] on the $\vec{\gamma}\vec{d} \to \pi NN$ reaction in the framework of the diagrammatic model built in Ref. [16]. In that work, we restricted ourselves to the discussion of unpolarized and single spin-dependent observables due to the lack of data on double spin-dependent observables at the time when the work was being prepared. It was found that the model [16] provided a quite satisfactory description of all available data except for the unpolarized differential and total cross sections in the $\gamma d \to \pi^0 np$ channel for which the data were notably overestimated. In the present work, we compare predictions of the approach [16] to the polarized data from Refs. [9–11] with special emphasis on the model dependence of our results. Sources for theoretical uncertainties are discussed in Ref. [16], to which the interested reader is referred.

Another principal goal of this work is to evaluate the contribution from the $\gamma d \to \pi NN$ channel to the deuteron GDH integral. This task requires an extension of the model up to about 1.5–2 GeV. Although in Ref. [16] we restricted our consideration to the Δ resonance region, the model is applicable at higher energies, too. As was shown in Ref. [17], one can expect that in the framework of the diagrammatic approach, contributions due to NN and πN final state interaction (FSI) are reliably calculated up to a photon energy of 800 MeV. Taking into account that these contributions are small above 500 MeV, they can obviously be disregarded for $E_\gamma \gtrsim 800$ MeV. Hence, the upper limit for the applicability of the model depends on that for the impulse approximation (IA) which, in turn, depends on the applicability domain of an employed elementary operator $\gamma N \to \pi N$ of pion production on the nucleon. In the framework of the approach [16], this operator is taken from multipole analyses SAID [18–20] and MAID [21] and can be used up to 2 GeV for the first analysis and up to 1.65 GeV for the second one.

The contribution from the $\gamma d \to \pi NN$ channel to the GDH integral up to $E_\gamma = 1.5$ GeV was evaluated in the AFS approach [13], but the sensitivity of obtained results to the $\gamma N \to \pi N$ operator was not investigated in that work. An analysis of Ref. [15] shows that the value of the integral at integration up to 350 MeV manifests its considerable dependence on the elementary operator. Because the energy domain from threshold to 350 MeV provides only about a half of the total contribution of this reaction to the deuteron GDH integral, it is of high interest to recognize how sensitive the total integral is to the $\gamma N \to \pi N$ operator. In the present paper, we evaluate the integral up to a photon energy of $E_\gamma = 1.65$ GeV and investigate a question of possible theoretical uncertainties for its value.

The work is organized as follows. In Sec. II, the kinematic relations used in the calculations as well as definitions for observables are reviewed. A brief description of the theoretical model and its ingredients is given in Sec. III. Section IV contains results for the unpolarized and helicity-dependent yields and cross sections and their comparison with the data available in the considered kinematic region. Results of the evaluation of the $\gamma d \to \pi NN$ channel contribution to the deuteron GDH integral are also given in Sec. IV. In Sec. V, we summarize the main conclusions and results.

II. KINEMATICS

Actual calculations of the reaction amplitude and observables are done in the laboratory frame where $k = (E_\gamma, \vec{k})$, $p_d = (M, \vec{0})$, $p_\pi = (\varepsilon_\pi, \vec{q})$, $p_1 = (\varepsilon_1, \vec{p}_1)$, and $p_2 = (\varepsilon_2, \vec{p}_2)$ are the four-momenta of the initial photon and deuteron and the final pion and nucleons, respectively. For the case when the final pion is detected, we take as independent kinematic variables the photon energy E_γ, the value of the pion momentum $q = |\vec{q}|$, the pion polar angle Θ_π, and the solid angle $\Omega_{\vec{P}_{NN}}$ ($\Theta_{\vec{P}_{NN}}$, $\phi_{\vec{P}_{NN}}$) of the relative momentum $\vec{P}_{NN}$ of the final nucleon-nucleon pair. These variables totally determine the kinematics.

The unpolarized differential cross section is given by

$$\frac{d\sigma}{d\vec{q}d\Omega_{\vec{P}_{NN}}} = f_{NN} \ \frac{1}{6} \sum_{m_2 m_1 \lambda m_d} |\langle m_2 m_1 | T | \lambda m_d \rangle|^2, \tag{2}$$

where $\langle m_2 m_1 | T | \lambda m_d \rangle$ is the reaction amplitude, and the phase space factor is

$$f_{NN} = \frac{1}{(2\pi)^5} \ \frac{m^2 |\vec{P}_{NN}|}{4 E_\gamma \varepsilon_\pi W_{NN}}, \tag{3}$$

with $W_{NN} = \sqrt{(p_1 + p_2)^2}$ and m is the nucleon mass. Spin states of the two nucleons and deuteron are m_2, m_1, and m_d, respectively, and they are chosen with respect to the z axis, which is defined by the photon momentum $\vec{k}$. The symbol λ stands for the photon helicity. An extra factor of 1/2 must be included in the rhs of Eq. (3) in the case of charged pion production.

We will be also interested in double polarized observables for the polarized photon beam and polarized deuteron target. These are the parallel, P, and antiparallel, A, cross sections defined as

$$\frac{d\sigma_P}{d\vec{q}d\Omega_{\vec{P}_{NN}}} = f_{NN} \ \frac{1}{2} \sum_{m_2 m_1} \Big(|\langle m_2 m_1 | T | + 1 + 1 \rangle|^2 + |\langle m_2 m_1 | T | - 1 - 1 \rangle|^2 \Big), \tag{4}$$

$$\frac{d\sigma_A}{d\vec{q}d\Omega_{\vec{P}_{NN}}} = f_{NN} \ \frac{1}{2} \sum_{m_2 m_1} \Big(|\langle m_2 m_1 | T | + 1 - 1 \rangle|^2 + |\langle m_2 m_1 | T | - 1 + 1 \rangle|^2 \Big). \tag{5}$$

To obtain the semi-inclusive differential cross sections $d\sigma/d\Omega_\pi$, $d\sigma_P/d\Omega_\pi$, and $d\sigma_A/d\Omega_\pi$, the right-hand sides of Eqs. (2), (4), and (5) have to be integrated over q and the solid angle $\Omega_{\vec{P}_{NN}}$, i.e.,

$$\frac{d\sigma}{d\Omega_\pi} = \int_{q^{\min}}^{q^{\max}} f_{NN} \ q^2 dq \int d\Omega_{\vec{P}_{NN}} \ \frac{d\sigma}{d\vec{q}d\Omega_{\vec{P}_{NN}}}, \tag{6}$$

$$\frac{d\sigma_P}{d\Omega_\pi} = \int_{q^{\min}}^{q^{\max}} f_{NN} \ q^2 dq \int d\Omega_{\vec{P}_{NN}} \ \frac{d\sigma_P}{d\vec{q}d\Omega_{\vec{P}_{NN}}}, \tag{7}$$

$$\frac{d\sigma_A}{d\Omega_\pi} = \int_{q^{\min}}^{q^{\max}} f_{NN} \ q^2 dq \int d\Omega_{\vec{P}_{NN}} \ \frac{d\sigma_A}{d\vec{q}d\Omega_{\vec{P}_{NN}}}. \tag{8}$$

The upper and lower integration limits in the laboratory frame are defined by the following relations

$$q^{\max} = q^{\max}(\Theta_\pi) = \frac{1}{b} \left[a E_\gamma z_\pi + (E_\gamma + M) \sqrt{a^2 - b\mu^2} \ \right], \tag{9}$$

$$q^{\min} = q^{\min}(\Theta_\pi) = \max\Big\{0, \ \frac{1}{b} \left[a E_\gamma z_\pi - (E_\gamma + M) \sqrt{a^2 - b\mu^2} \ \right] \Big\}, \tag{10}$$

where $a = (W_{\gamma d}^2 - 4m^2 + \mu^2)/2$, $b = (E_\gamma + M)^2 - E_\gamma^2 z_\pi^2$, $z_\pi = \cos\Theta_\pi$, and μ is the pion mass.

For the neutral channel, the emitted proton was registered in the experiment [11]. In this case we chose as independent kinematic variables the photon energy E_γ, the value of the proton momentum $p_p = |\vec{p}_p|$, the proton polar angle Θ_p, and the solid angle $\Omega_{\vec{P}_{\pi n}}$ $(\Theta_{\vec{P}_{\pi n}}, \phi_{\vec{P}_{\pi n}})$ of the relative momentum $\vec{P}_{\pi n}$ of the final meson-neutron pair. Equations analogous to Eqs. (9) and (10) are now of the form

$$p_p^{\max} = p_p^{\max}(\Theta_p) = \frac{1}{B}\left[AE_\gamma z_p + (E_\gamma + M)\sqrt{A^2 - Bm^2}\,\right], \tag{11}$$

$$p_p^{\min} = p_p^{\min}(\Theta_p) = \max\Big\{0,\ \frac{1}{B}\left[AE_\gamma z_p - (E_\gamma + M)\sqrt{A^2 - Bm^2}\,\right]\Big\}, \tag{12}$$

where $A = (W_{\gamma d}^2 - 2m\mu - \mu^2)/2$, $B = (E_\gamma + M)^2 - E_\gamma^2 z_p^2$, and $z_p = \cos\Theta_p$.

Only a fraction of the total interval $[p_p^{\min}, p_p^{\max}]$ was accessed in conditions of the experiment [11]. There were registered the protons with the absolute value of the momentum $p_p \geq p_{\rm exp}^{\min}$, where

$$p_{\rm exp}^{\min} = p_{\rm exp}^{\min}(\Theta_p) = [210 + 0.01 \times (\Theta_p - 90^\circ)^2]\ {\rm MeV}/c, \tag{13}$$

so that the differential $\pi^0 np$ yields Y, as they were called in Ref. [11], were measured rather than the differential cross sections. In analogy to Eqs. (6)–(8) they are defined as

$$\frac{dY}{d\Omega_p} = \int_{p_{\rm exp}^{\min}}^{p_p^{\max}} f_{\pi n}\ p_p^2\ dp_p \int d\Omega_{\vec{P}_{\pi n}}\ \frac{1}{6} \sum_{m_p m_n \lambda m_d} |\langle m_p m_n | T | \lambda m_d \rangle|^2, \tag{14}$$

$$\frac{dY_P}{d\Omega_p} = \int_{p_{\rm exp}^{\min}}^{p_p^{\max}} f_{\pi n}\ p_p^2\ dp_p \int d\Omega_{\vec{P}_{\pi n}}\ \frac{1}{2} \sum_{m_p m_n} \Big(|\langle m_p m_n | T | + 1 + 1 \rangle|^2 + |\langle m_p m_n | T | - 1 - 1 \rangle|^2\Big), \tag{15}$$

$$\frac{dY_A}{d\Omega_p} = \int_{p_{\rm exp}^{\min}}^{p_p^{\max}} f_{\pi n}\ p_p^2\ dp_p \int d\Omega_{\vec{P}_{\pi n}}\ \frac{1}{2} \sum_{m_p m_n} \Big(|\langle m_p m_n | T | + 1 - 1 \rangle|^2 + |\langle m_p m_n | T | - 1 + 1 \rangle|^2\Big), \tag{16}$$

where

$$f_{\pi n} = \frac{1}{(2\pi)^5}\ \frac{m^2 |\vec{P}_{\pi n}|}{4 E_\gamma \varepsilon_p W_{\pi n}}, \tag{17}$$

and $W_{\pi n} = \sqrt{(p_\pi + p_n)^2}$.

III. THE FORMALISM

In this section we briefly outline the formalism used to evaluate the $\gamma d \to \pi NN$ reaction amplitude. It was described in Refs. [16, 22, 23], to which the reader is referred for more details. The diagrammatic approach is exploited to calculate the $\gamma d \to \pi NN$ reaction amplitude. Because in this work we are not interested in the threshold region, we reduce the set of diagrams in comparison to that considered in Ref. [23]. Specifically, only contributions from the three diagrams shown in Figs. 1(a)–(c) to the reaction amplitude have been taken into account. Diagram 1(a) is often refereed to as IA. Sometimes it is called the pole diagram. Apart from it, the diagrams 1(b) and (c) corresponding, respectively, to NN and πN rescattering in the final state have been considered in the present calculation.

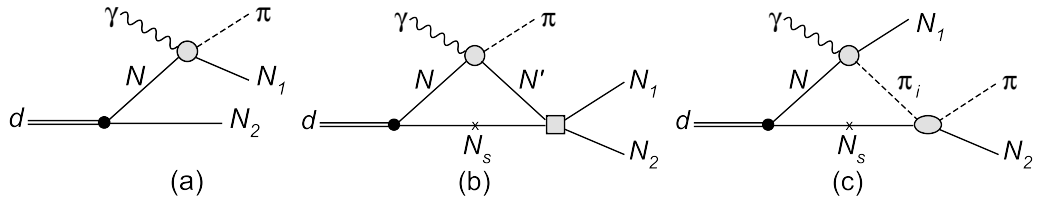

FIG. 1: Diagrammatic representation of the $\gamma d \to \pi NN$ amplitude. Diagram (a) corresponds to IA. Mechanisms with NN and πN rescattering in the final state are shown in diagrams (b) and (c), respectively. Diagrams with the permutation $N_1 \leftrightarrow N_2$ are not shown. The spectator nucleon indicated by an x is on-shell.

One remark should be made here. A detailed analysis of the helicity dependence of the $\vec{\gamma}\vec{d} \to \pi NN$ reaction up the $\Delta(1232)$ resonance is presented in Ref. [15]. Special attention was given in that work to the near-threshold region. Within the approach [15] the same set of diagrams as presented in Fig. 1 was taken into account. One can expect such a model to be quite realistic near threshold for the description of the charged channels. But this is not obviously to be the case for the neutral channel. As was shown in Ref. [23], a two-loop diagram as in Fig. 2(a) which includes simultaneously πN rescattering in the intermediate state and np rescattering in the final state has to be taken into account at threshold energies. A similar mechanism is known to be very important near threshold for coherent π^0 photoproduction on the deuteron $\gamma d \to \pi^0 d$ [24–26].

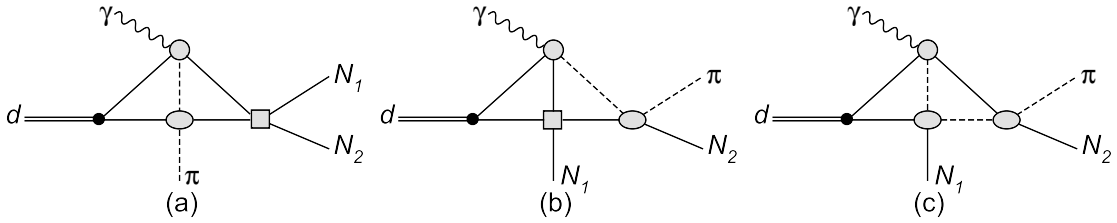

FIG. 2: Two-loop diagrams of the reaction $\gamma d \to \pi NN$. The permutation $N_1 \leftrightarrow N_2$ is not shown.

The importance of diagram (a) in Fig. 2 at threshold energies is that it contains, together with the np scattering amplitude, a block with charged pion photoproduction from the nucleon. The dominating threshold electric dipole amplitude E_{0+} for the charged channels is about 20 times larger in absolute numbers than that for the neutral channels. For analogous reasons we also expect that a two-loop diagram 2(b) with NN rescattering in the intermediate state and πN rescattering in the final state may also be important near threshold. Therefore, the fact that the model including only three contributions shown in Figs. 1(a)–(c) can be used for the description of the $\gamma d \to \pi^0 np$ reaction at threshold energies is not obvious, and further study is needed to clarify this point. There is one more two-loop diagram, shown in Fig. 2(c), which includes two blocks with πN scattering. Because the πN scattering lengths are about two orders smaller than those for NN scattering, the role of this diagram in the threshold region is expected to be much smaller than that of diagrams 2(a) and 2(b).

One can anticipate the effect from the above two-loop diagrams to decrease together with increasing E_γ when the mentioned enhancement due to the charge pion exchange disappears. Nevertheless, to be fully confident in the smallness of such contributions, their explicit evaluations are needed. This task, however, is expected to be very difficult, because as we have learned evaluating diagram 2(a) in Ref. [23], practical calculations are extremely time consuming especially when the inclusive processes are considered, and, therefore, integrations over momenta of final particles have to be carried out. Note that in the case of the exclusive channels, the kinematic regions exist where the diagrams in Figs. 1(a)–1(c) can be suppressed, and other mechanisms, in particular, the two-loop diagrams 2(a)–2(c) become important and have to be taken into account (see Refs. [27, 28] for detailed discussions of this point).

Let us now write explicit expressions for the amplitudes corresponding to diagrams 1(a)–1(c). One has for the IA amplitude

$$\langle m_2 m_1 | T^{\rm IA}(\vec{p}_2, \vec{p}_1, \vec{q}; \vec{k}) | \lambda m_d \rangle = \sum_m \Psi^{m_d}_{m_2 m}(\vec{p}_2)\, \langle m_1 | T_{\gamma N \to \pi N_1}(\vec{p}_1, \vec{q}; \vec{k}) | \lambda m \rangle, \tag{18}$$

where $\Psi^{m_d}_{m_2 m}$ is the deuteron wave function having the form

$$\Psi^{m_d}_{m_2 m_1}(\vec{p}) = \sum_{L=0,2} i^L C^{1 m_S}_{\frac{1}{2} m_2 \frac{1}{2} m_1} C^{1 m_d}_{1 m_S L m_L} Y^{m_L}_L(\hat{\vec{p}}) u_L(p). \tag{19}$$

In Eq. (19), $Y^{m_L}_L(\hat{\vec{p}})$ are the spherical harmonics, and $C^{JM}_{J_1 M_1 J_2 M_2}$ are the Clebsch-Gordan coefficients. The S and D wave function amplitudes $u_0(p)$ and $u_2(p)$ are taken for the CD-Bonn potential [29]. One should emphasize that calculations with another realistic version of the nucleon-nucleon potential, namely, with the Nijmegen model [30], have led to essentially the same results, so we have found no sensitivity of our predictions to the choice of a potential. Note that in Eq. (18) and in the amplitudes that follow, we do not write explicitly those corresponding to the permutation $N_1 \leftrightarrow N_2$, but they are included in the calculations.

The symbol $T_{\gamma N \to \pi N}$ in Eq. (18) stands for the elementary operator of pion photoproduction on the nucleon. As is explained in detail in Ref. [16] (see, also Ref. [11]), ambiguities in predictions for observables in the $\gamma d \to \pi NN$ reaction stem mainly from the manner in which $T_{\gamma N \to \pi N}$ is embedded into the deuteron. In all recent calculations [15–17], this operator is taken in the on-shell form and it is parameterized using either the multipole analyses SAID [18]

and MAID [21] or the effective Lagrangian approach (ELA) [31]. Although the models are close in their predictions for observables in the reaction $\gamma N \to \pi N$, they are not identical. It is evident that this difference will manifest itself in results of the evaluation of Eq. (18). To estimate ambiguities caused by different choices of the on-shell operator $T_{\gamma N\to\pi N}$, we perform our calculations with the latter taken from the recent multipole analyses SAID [18] (solution SP09K) and MAID07 [32].

Furthermore, the on-shell operator $T_{\gamma N\to\pi N}$ depends on four invariant amplitudes [33] for which there exist different options that are equivalent in the on-shell case. This equivalence is broken when one or both nucleons are off their mass shells. Just such a situation takes place in Eq. (18) where the nucleon N is off its mass shell. In this work, we evaluate the operator $T_{\gamma N\to\pi N}$ with two sets of the invariant amplitudes, A_i and A'_i, as they are called in Ref. [16] and where their definition can be found. At least, this allows one to estimate the possible uncertainties in the predicted observables due to off-shell effects in $T_{\gamma N\to\pi N}$.

The matrix element corresponding to Fig. 1(b) reads

$$\begin{aligned}\langle m_2 m_1|T^{NN}(\vec{p}_2,\vec{p}_1,\vec{q};\vec{k})|\lambda m_d\rangle &= m\int\frac{d^3\vec{p}_s}{(2\pi)^3}\frac{1}{p^2_{\rm out}-p^2_{\rm in}+i0}\\ &\times\sum_{m_s m'}\langle\vec{p}_{\rm out},m_2 m_1|T_{NN}(E)|\vec{p}_{\rm in},m_s m'\rangle\langle m_s m'|T^{\rm IA}(\vec{p}_s,\vec{p}\,',\vec{q};\vec{k})|\lambda m_d\rangle. \qquad (20)\end{aligned}$$

Here $T^{\rm IA}$ is the IA amplitude given by Eq. (18). The relative momenta of the N_2N_1 pair after and before scattering are $\vec{p}_{\rm out}=(\vec{p}_2-\vec{p}_1)/2$ and $\vec{p}_{\rm in}=\vec{p}_s-(\vec{p}_2+\vec{p}_1)/2$, respectively, and $E=p^2_{\rm out}/m$. The half-off-shell NN scattering matrix T_{NN} has been obtained by solving an equation of the Lippmann-Schwinger type for the CD-Bonn potential [29]. All states with the total angular momentum $J\le 2$ have been retained in T_{NN}.

In the evaluation of Eq. (20) there is another ambiguity due to different prescriptions for the determination of the total invariant energy entering the γN vertex. As was proposed in Refs. [27, 28], we define the latter as if the spectator nucleon N_s was on its mass-shell. Other prescriptions can also be found in the literature. For instance, in Ref. [17] the active nucleon N is put to be on its mass-shell. We have evaluated Eq. (20) with these two prescriptions and found only at most a 2% variation for all observables considered in the next section. This means that the above ambiguity can be safely disregarded.

The matrix element corresponding to Fig. 1(c) with πN rescattering in the final state is

$$\begin{aligned}\langle m_2 m_1|T^{\pi N}(\vec{p}_2,\vec{p}_1,\vec{q};\vec{k})|\lambda m_d\rangle &= \int\frac{d^3\vec{p}^{\,*}_s}{(2\pi)^3}\,\frac{\varepsilon^*_2+\varepsilon^*_s}{2W_{\pi N_2}}\,\frac{1}{\vec{p}^{\,*2}_2-\vec{p}^{\,*2}_s+i0}\,F^2_{\pi N}(|\vec{q}_{\pi_i}|)\\ &\times\sum_{m_s}\Big[\langle\vec{p}^{\,*}_2,m_2|T^0_{\pi N}(W_{\pi N_2})|\vec{p}^{\,*}_s,m_s\rangle\langle m_s m_1|T^{\rm IA}_{\pi^0 N_1}(\vec{p}_s,\vec{p}_1,\vec{q}_{\pi_i};\vec{k})|\lambda m_d\rangle \qquad (21)\\ &-\langle\vec{p}^{\,*}_2,m_2|T^{\rm ch}_{\pi N}(W_{\pi N_2})|\vec{p}^{\,*}_s,m_s\rangle\langle m_s m_1|T^{\rm IA}_{\pi^{\rm ch} N_1}(\vec{p}_s,\vec{p}_1,\vec{q}_{\pi_i};\vec{k})|\lambda m_d\rangle\Big],\end{aligned}$$

where the asterisk denotes variables in the πN_2 center-of-mass (c.m.) frame, i.e. $\vec{p}^{\,*}_s=-\vec{q}^{\,*}_\pi$, where $\vec{p}^{\,*}_s$ and $\vec{q}^{\,*}_\pi$ are the c.m. initial nucleon and pion momenta, respectively, in the πN scattering vertex. Analogously, $\vec{p}^{\,*}_2=-\vec{q}^{\,*}$, where $\vec{p}^{\,*}_2$ and $\vec{q}^{\,*}$ are the c.m. final nucleon and pion momenta, respectively. The momenta with the asterisk and without it are related to each other through a boost transformation with the velocity $(\vec{q}+\vec{p}_2)/(\varepsilon_\pi+\varepsilon_2)$. We take the spectator nucleon N_s to be on its mass shell, i.e. $\varepsilon^*_s=\sqrt{p^{*2}_s+m^2}$. The total energy $W_{\pi N_2}$ of the πN_2 pairs is $W_{\pi N_2}=\sqrt{(q+p_2)^2}=\varepsilon^*_2+\varepsilon^*_\pi=\sqrt{\vec{p}^{\,*2}_2+m^2}+\sqrt{\vec{q}^{\,*2}+\mu^2}$.

The half-off-shell πN scattering matrix $T_{\pi N}$ has been obtained by solving the Lippmann-Schwinger equation for a separable energy-dependent πN potential built in Ref. [34]. We have checked that the results remain essentially the same as the $T_{\pi N}$ found from a meson-exchange model [35, 36]. The factor $F^2_{\pi N}(|\vec{q}_{\pi_i}|)$ in Eq. (21) is introduced to take into account the off-shell nature of the intermediate meson π_i. In accordance with Ref. [34], we choose the form factor $F_{\pi N}(q)$ of the πNN vertex to be of the monopole form

$$F_{\pi N}(q)=\frac{\Lambda^2_\pi}{\Lambda^2_\pi+q^2}, \qquad (22)$$

with a cutoff parameter $\Lambda_\pi=650$ MeV/c.

The superscript indices "0" and "ch" in the $T_{\pi N}$ amplitude in Eq. (21) stand for the neutral, $\pi^0 N\to\pi^0 N_1$, or charge exchange, $\pi^{\rm ch}N\to\pi^0 N_1$, channels, respectively. The IA amplitudes for π^0 photoproduction, $T^{\rm IA}_{\pi^0 N_1}$, and for charged pion photoproduction, $T^{\rm IA}_{\pi^{\rm ch} N_1}$, are given by Eq. (18).

IV. RESULTS AND DISCUSSION

A. Unpolarized yield and cross section

We begin the discission of the results with the unpolarized yield and cross section. Special emphasize is given to their comparison with the very recent experimental data from Refs. [9–11]. A detailed comparison with older data can be found in Ref. [16]. As a rule, we will not compare our predictions with the results of other theoretical approaches [15, 17, 37] because this has already been done in Ref. [11].

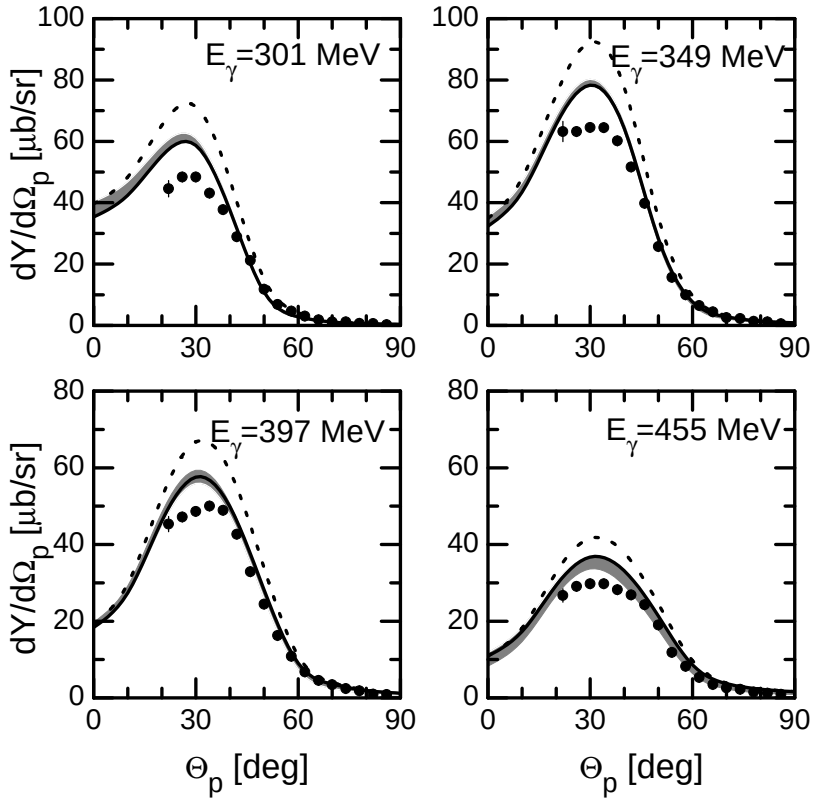

FIG. 3: Unpolarized differential yield for the $\gamma d \to \pi^0 np$ reaction at four selected energies. Dotted and solid curves are obtained in IA and the full model, respectively, with the MAID07 analysis and the amplitudes A_i. Shaded areas are our predictions with different parameterizations of the elementary $\gamma N \to \pi N$ amplitude as described in the text. Data are from Ref. [11]. Only statistical errors are shown.

Results for the unpolarized differential yield (14) for the $\gamma d \to \pi^0 np$ reaction at four selected energies from 301 to 455 MeV with a step of about 50 MeV are shown in Fig. 3. One can see a sizable effect from FSI, which is mainly due to np FSI. The yield is reproduced very well at the proton angles $\Theta_p \geq 40°$. However, despite of the strong reduction of the unpolarized differential yield due to FSI, the full model clearly overestimates the data in the peak position. An analogous feature was found also in Ref. [16] where after integration over complete acceptance, i.e. with $p_p^{\min}$ given by Eq. (12), we observed the predictions to lie well above data from Refs. [7, 38]. Similar overestimation, although in some variation of size, is present in all recent calculations [17, 37, 39].

It is difficult to find a reasonable explanation for this disagreement in the framework of the present model. First, reasons for a possible failure of the IA calculation are not apparent. The contribution of IA to the total cross section stems from the quasi-free $\pi^0 N$ process, which is evaluated very reliably. Second, as explained in Ref. [16], the NN FSI contribution comes mainly from the kinematic domains where nucleons N and N' in Fig. 1(b) are close to their mass shells so that the on-shell parameterization of the elementary operator $T_{\gamma N \to \pi N}$ can be used in Eq. (20). Because modern parameterizations of $T_{\gamma N \to \pi N}$ and T_{NN} are firmly established, we think that the effect of NN FSI is well under control. Therefore, the noticeable disagreement with the data cannot be explained by an underestimation of the NN FSI contribution. We also suppose that πN FSI is evaluated quite reasonably and it can not be responsible for the disagreement, especially if one takes into account that the πN FSI effect is very small.

As discussed in Refs. [11, 37], a possible way to resolve the problem is to take into account the absorption of the

produced pions by the pair of nucleons. Rough estimations of the absorption effect performed in Ref. [11] show that it can comprise more than 10% of the total cross section, thus leading to visible attenuation of the production rate.

Model uncertainties of the predictions stemming from the choice of the elementary operator $T_{\gamma N\to\pi N}$ are shown in the shaded areas in Fig. 3. These areas have been generated, first, by results with the MAID07 and SAID (solution SP09K) multipole analyses and, second, with two sets of the invariant amplitudes, A_i and A'_i, as described in the previous section. One can see that the model dependence is quite small, and even when taken into account, it does not resolve the problem with the description of the data at $\Theta_p \leq 40^\circ$.

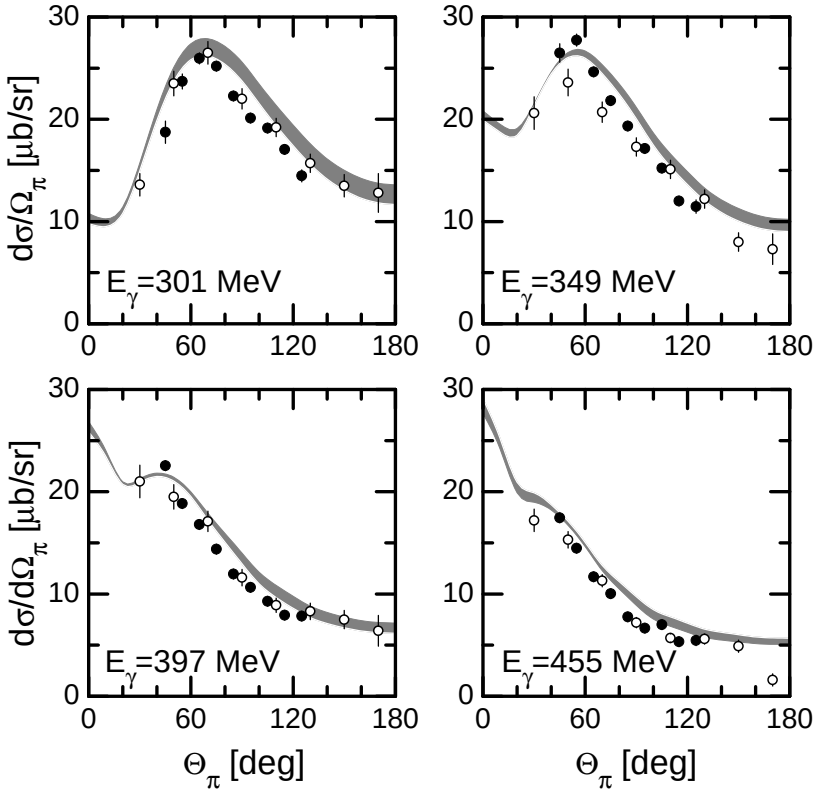

FIG. 4: Unpolarized differential cross section for the $\gamma d \to \pi^- pp$ reaction at four selected energies. Shaded areas are our predictions with different parameterizations of the elementary $\gamma N \to \pi N$ amplitude. Data are from Refs. [11] (•) and [40] (○). Only statistical errors are shown.

Predictions for the unpolarized differential cross section in the $\gamma d \to \pi^- pp$ reaction are compared in Fig. 4 to the data from Refs. [11, 40] at the same energies as in Fig. 3. The agreement is quite reasonable, although the slight overestimation of the data is seen. The model dependence of the predictions is mainly due to the choice of the multipole analysis and is noticeable only at the lowest energy. It is compatible with the data errors of Ref. [40]. Together with increasing E_γ this dependence diminishes and becomes quite small above 350 MeV.

As is seen in Fig. 5, the agreement of the predictions and the unpolarized $\pi^+ nn$ data is almost perfect. Again, the visible dependence of the results on the choice of the multipole analysis occurs only at 301 MeV.

Taking into account the results for the unpolarized differential cross sections in the charged channels, one could expect the sum of the total cross sections for these two channels to be in reasonable agreement with the data but with a possible slight overestimation because of the above overestimation in the $\pi^- pp$ reaction. However, as is seen in Fig. 6, the deviation from the data of the GDH and A2 collaborations [9] at $E_\gamma \geq 300$ MeV is more serious. At present, we are not aware of reasons for this disagreement. Figure 6 shows also that our results are in good agreement with these of AFS up to the peak position at about 320 MeV, but at higher energies our cross sections overestimate the AFS results.

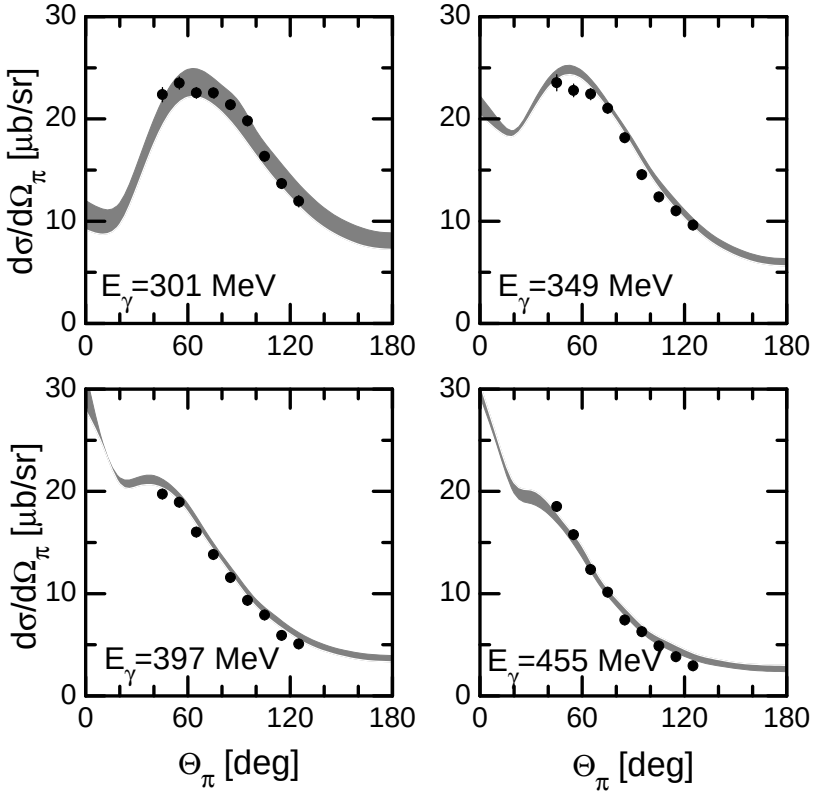

FIG. 5: Same as Fig. 4, but for the $\gamma d \to \pi^+ nn$ reaction.

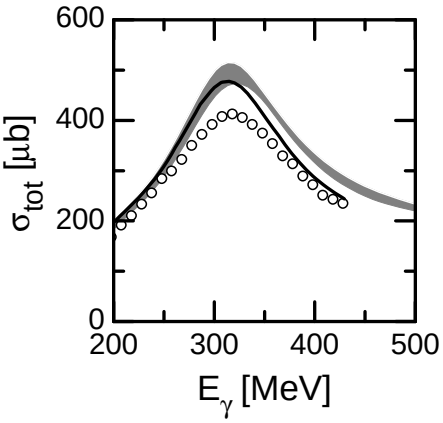

FIG. 6: Unpolarized total cross section for the charged channels $\gamma d \to \pi^{\pm} NN$. Shaded area is our predictions with different parameterizations of the elementary $\gamma N \to \pi N$ amplitude. Solid curve is the AFS result [13]. Data are from Ref. [9].

B. Polarized yield and cross section

Next we discuss the polarized yield and cross section. Figure 7 shows the helicity-dependent yield difference

$$\frac{\Delta Y}{d\Omega_p} = \frac{dY_P}{d\Omega_p} - \frac{dY_A}{d\Omega_p} \tag{23}$$

for the $\pi^0 np$ channel. Similar to the unpolarized yield, one can see a sizable reduction of $\Delta Y/d\Omega_p$ in IA due to FSI. However, the striking distinction from the unpolarized case is that now the model reasonably reproduces all the data not only those at $\Theta_p \geq 40^\circ$. This might indicate that the above overestimation in the unpolarized yield is due to an overestimation in both $dY_P/d\Omega_p$ and $dY_A/d\Omega_p$, but it disappears in the difference $\Delta Y/d\Omega_p$.

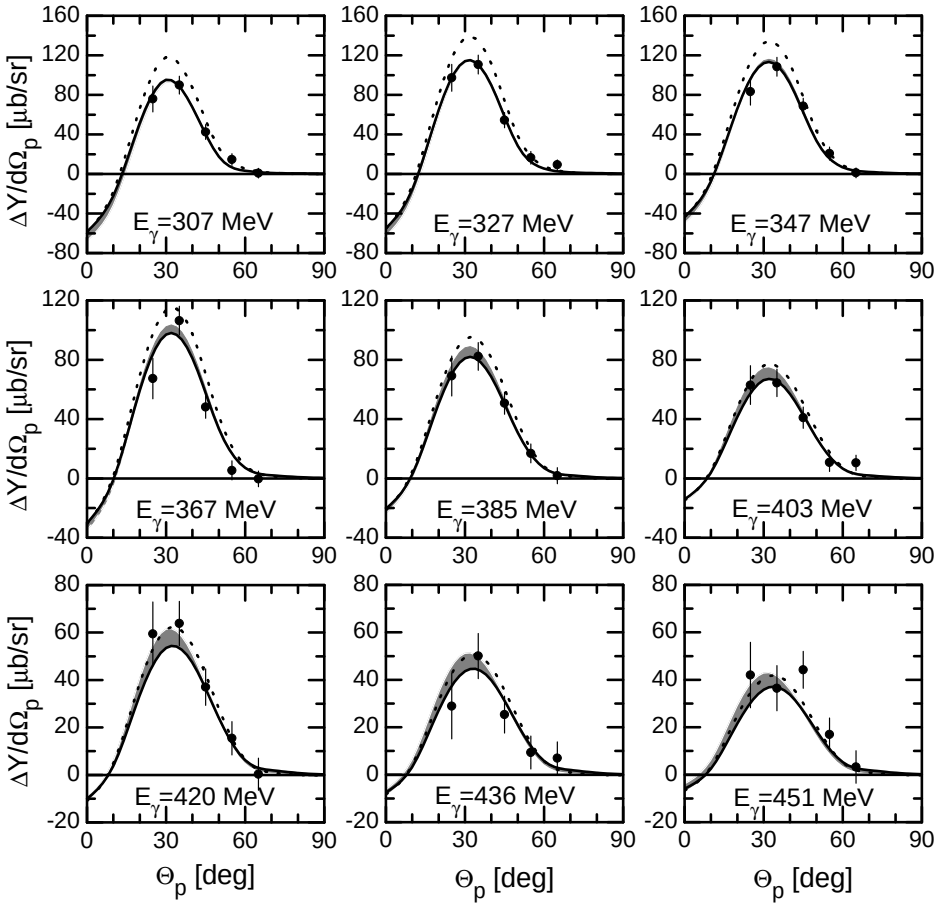

FIG. 7: Helicity-dependent differential yield difference $\Delta Y/d\Omega_p$ for the $\gamma d \to \pi^0 np$ reaction. Dotted and solid curves are obtained in IA and the full model, respectively, with the amplitudes A_i and the MAID07 analysis. Shaded areas are our predictions with different parameterizations of the elementary $\gamma N \to \pi N$ amplitude. Data are from Ref. [11]. Only statistical errors are shown.

It is seen in Fig. 7 that the dependence of $\Delta Y/d\Omega_p$ on the elementary operator is weak below 350 MeV, but it becomes quite visible at higher energies.

Figures 8 and 9 show the helicity-dependent differential cross section difference

$$\frac{\Delta\sigma}{d\Omega_\pi} = \frac{d\sigma_P}{d\Omega_\pi} - \frac{d\sigma_A}{d\Omega_\pi} \tag{24}$$

for the $\pi^- pp$ and $\pi^+ nn$ channels, respectively. There is a good agreement with our results within the uncertainties of the theoretical predictions. Only a few $\pi^- pp$ data points are underestimated at $\Theta_\pi = 125^\circ$. The above uncertainties are quite significant only in the $\pi^+ nn$ channel and just in the angular region overlapped in the experiment [11].

An integration of Eq. (24) over the solid angle Θ_π gives the difference $\Delta\sigma = \sigma_P - \sigma_A$ of the total cross sections. This difference for the semi-exclusive channels $\gamma d \to \pi^\pm NN$ and $\gamma d \to \pi^0 X$ has been measured in Refs. [9, 10] at energies from 200 to 430 MeV. Because we do not have a model for the coherent reaction $\gamma d \to \pi^0 d$, we are able to make predictions for the second channel. Our results for the $\pi^\pm NN$ channel are shown in Fig. 10. Within theoretical uncertainties, the model satisfactory describes the data of Ref. [9] below 300 MeV, but there exists noticeable overestimation at higher energies, i.e. one observes the situation analogous to that for the unpolarized cross section. Reasonable agreement with the data of Ref. [10] is achieved except for two points in the peak region. Our results are in quite good agreement with the AFS predictions but overestimate these from Ref. [37] at $E_\gamma \gtrsim 280$ MeV.

Having measured the unpolarized yield and cross section as well as $\Delta Y/d\Omega_p$ and $\Delta\sigma/d\Omega_\pi$, the authors of Ref. [11] have attempted to separate the parallel and antiparallel components of the yield and cross section. To do this, they

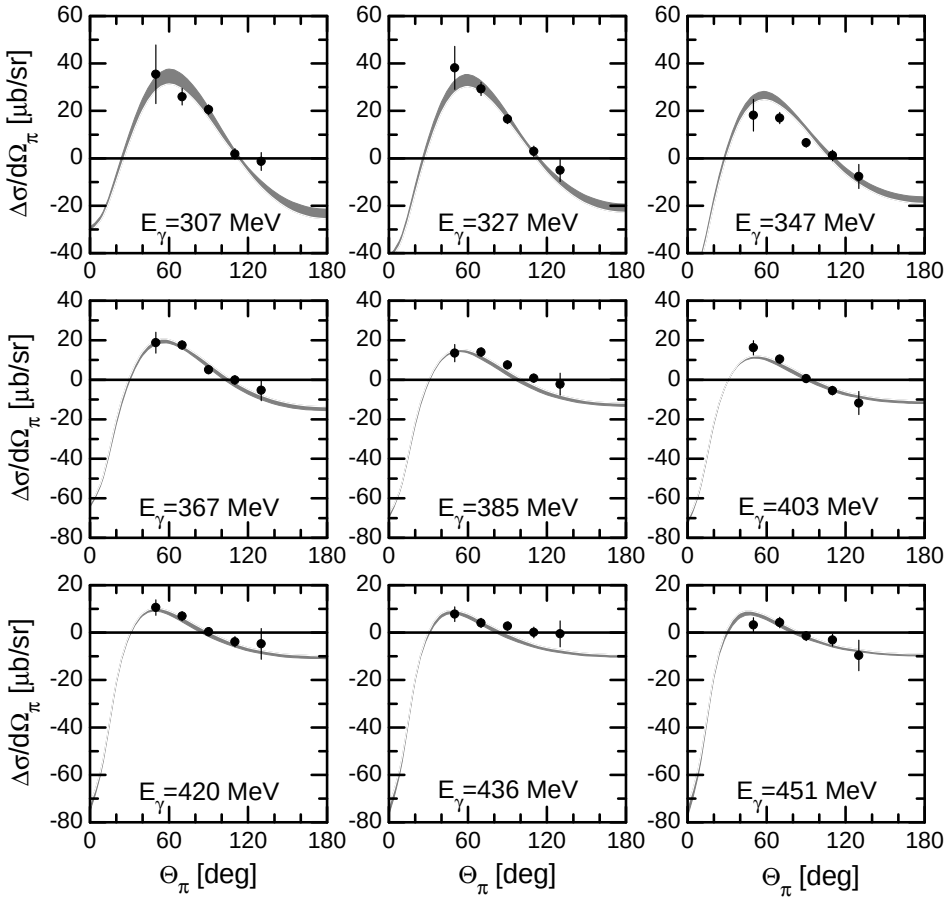

FIG. 8: Helicity-dependent differential cross section difference $\Delta\sigma/d\Omega_\pi$ for the $\gamma d \to \pi^- pp$ reaction. Shaded areas are our predictions with different parametrizations of the elementary $\gamma N \to \pi N$ amplitude. Data are from Ref. [11]. Only statistical errors are shown.

used the follows relations:

$$\frac{d\sigma}{d\Omega} = \frac{1}{3}\Big(2\frac{d\sigma_\parallel}{d\Omega} + \frac{d\sigma_0}{d\Omega}\Big), \tag{25}$$

$$T_{20}\frac{d\sigma}{d\Omega} = \frac{\sqrt{2}}{3}\Big(\frac{d\sigma_\parallel}{d\Omega} - \frac{d\sigma_0}{d\Omega}\Big), \tag{26}$$

where $\sigma_\parallel$ and σ_0 are the components of the cross section corresponding to the deuteron spin states $m_d = \pm 1$ and $m_d = 0$, respectively, and T_{20} is the tensor target asymmetry [16, 41]. Note that the component $\sigma_\parallel$ is the average of the parallel and antiparallel cross sections

$$\frac{d\sigma_\parallel}{d\Omega} = \frac{1}{2}\Big(\frac{d\sigma_P}{d\Omega} + \frac{d\sigma_A}{d\Omega}\Big). \tag{27}$$

It is follows from Eqs. (25) and (26) that

$$\frac{d\sigma}{d\Omega} = \frac{\sqrt{2}}{\sqrt{2}+T_{20}}\,\frac{d\sigma_\parallel}{d\Omega}. \tag{28}$$

Evaluations of T_{20} in Refs. [16, 17] showed that in the angular regions accessed in conditions of the experimental setup of Ref. [11], i.e. at $\Theta_\pi > 20^\circ$, the absolute value of T_{20} does not exceed 0.05. Therefore, one has the following approximate relations for $\Theta_\pi > 20^\circ$:

$$\frac{d\sigma}{d\Omega} \approx \frac{d\sigma_\parallel}{d\Omega}, \quad \frac{d\sigma_\parallel}{d\Omega} \approx \frac{d\sigma_0}{d\Omega}. \tag{29}$$

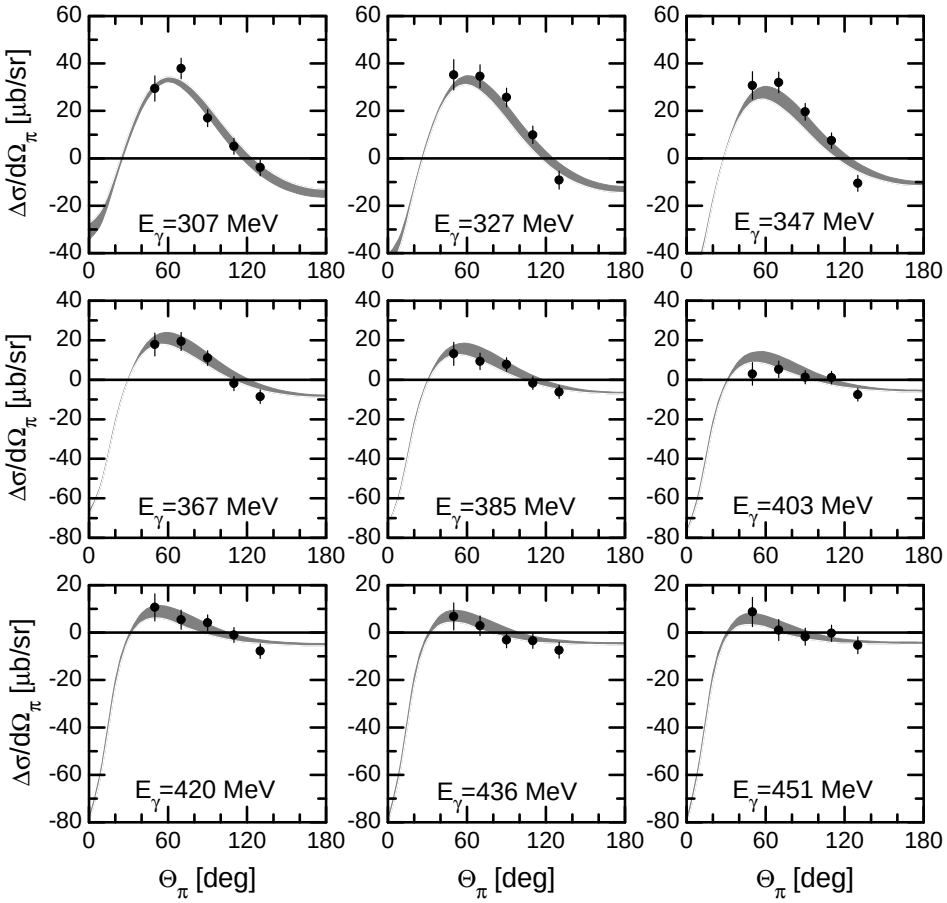

FIG. 9: Same as Fig. 8, but for the $\gamma d \to \pi^+ nn$ reaction.

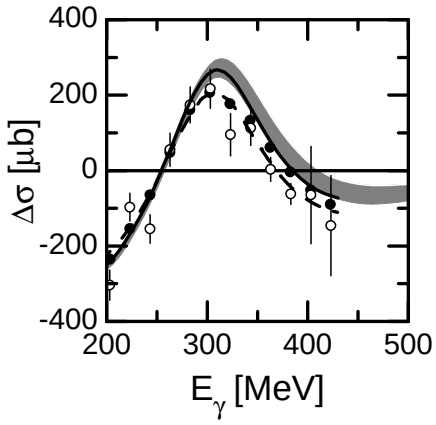

FIG. 10: Difference $\Delta\sigma$ for the charged channels $\gamma d \to \pi^{\pm} NN$. Shaded area is our predictions with different parametrizations of the elementary $\gamma N \to \pi N$ amplitude. Solid and dashed curves are the AFS [13] and Schwamb [37] results, respectively. Data are from Refs. [9] (○) and [10] (●). Only statistical errors are shown.

Using Eqs. (24), (25), (27), and (29) one obtains

$$\frac{d\sigma_{P/A}}{d\Omega} \approx \frac{d\sigma}{d\Omega} \pm \frac{1}{2}\frac{\Delta\sigma}{d\Omega}. \tag{30}$$

It should be noted that the semi-inclusive asymmetry T_{20} resulting from the integration of the corresponding right-hand sides over the kinematic regions appearing in Eqs. (14)–(16) was not evaluated in Refs. [16, 17]. However, we

have checked that such an integration gives $|T_{20}| \leq 0.08$ at $25^\circ \leq \Theta_p \leq 65^\circ$ and, therefore, the relations similar to Eqs. (29) and (30) are valid for the measured yields as well.

Figures 11–13 demonstrate our predictions for the parallel and antiparallel yields and cross sections. A comparison with the experimental results from Ref. [11] is also presented in these figures. One can see that the description of the data is quite reasonable, but not perfect. Such an agreement could be anticipated for the charged channels, but it is rather unexpected for the $\pi^0 np$ reaction. Currently, we are not aware of the reasons why the model that describes reasonably well the P and A components of the polarized yield, nevertheless, fails in reproducing the unpolarized yield.

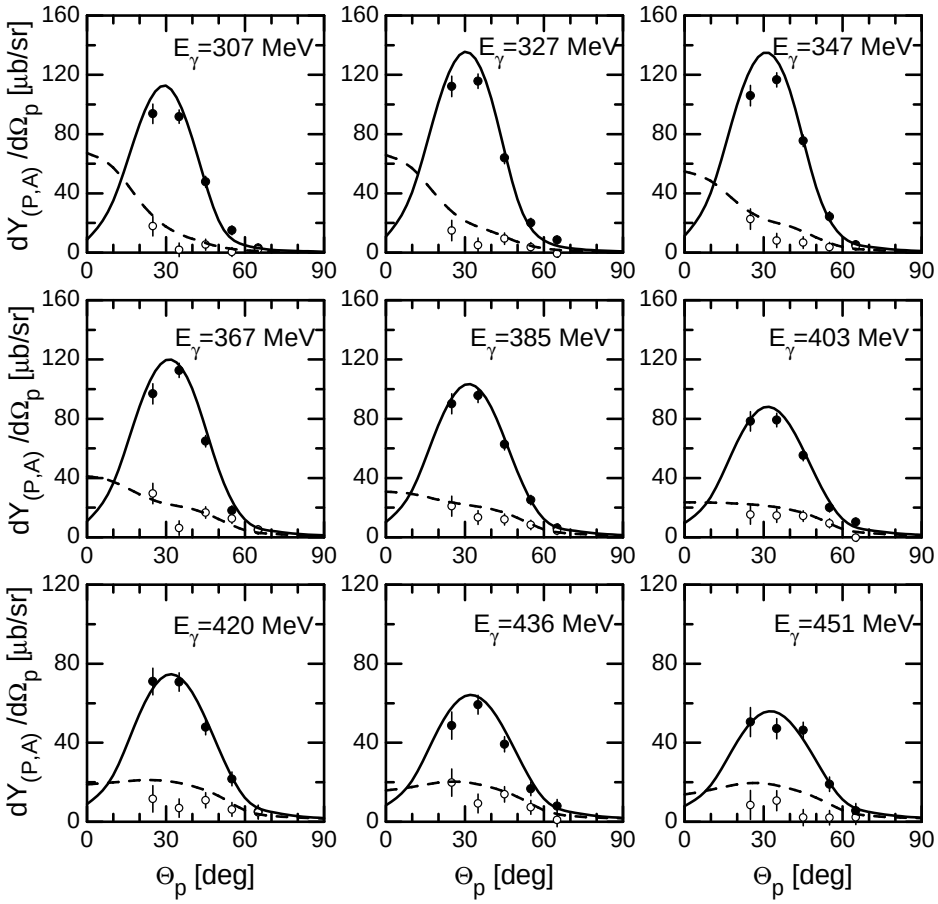

FIG. 11: Helicity-dependent differential yields $dY_P/d\Omega_p$ and $dY_A/d\Omega_p$ for the $\gamma d \to \pi^0 np$ reaction. Solid and dashed curves are our predictions for $dY_P/d\Omega_p$ and $dY_A/d\Omega_p$, respectively, with the amplitudes A_i and the MAID07 analysis. Data are from Ref. [11] for the parallel (•) and antiparallel (○) components. Only statistical errors are shown.

We do not discuss here the shape of the angular behavior of the P and A components in the yield and differential cross section because the corresponding analysis has already been performed in Ref. [11]. As shown in that work, this behavior can be interpreted in terms of pion photoproduction on single nucleons, and it is a consequence of the dominance of quasi-free reaction mechanisms.

C. The $\gamma d \to \pi NN$ contribution to the GDH integral for the deuteron

Let us discuss now the contribution of the $\gamma d \to \pi NN$ reaction to the deuteron GDH integral and compare our results with those obtained in Refs. [13, 15]. Figure 14 presents the difference $\Delta\sigma$ as a function of the photon energy E_γ for three channels. As was shown in Refs. [13, 15], the behavior of the difference repeats mainly that for the elementary reaction $\gamma N \to \pi N$ with some distortion due to nuclear effects. For instance, the negative value of $\Delta\sigma$ in the charged channels at threshold energies is because of the dominance of the E_{0+} multipole producing the antiparallel transition. The M_{1+} multipole provides the strong positive value in the Δ region that Fig. 14 clearly demonstrates.

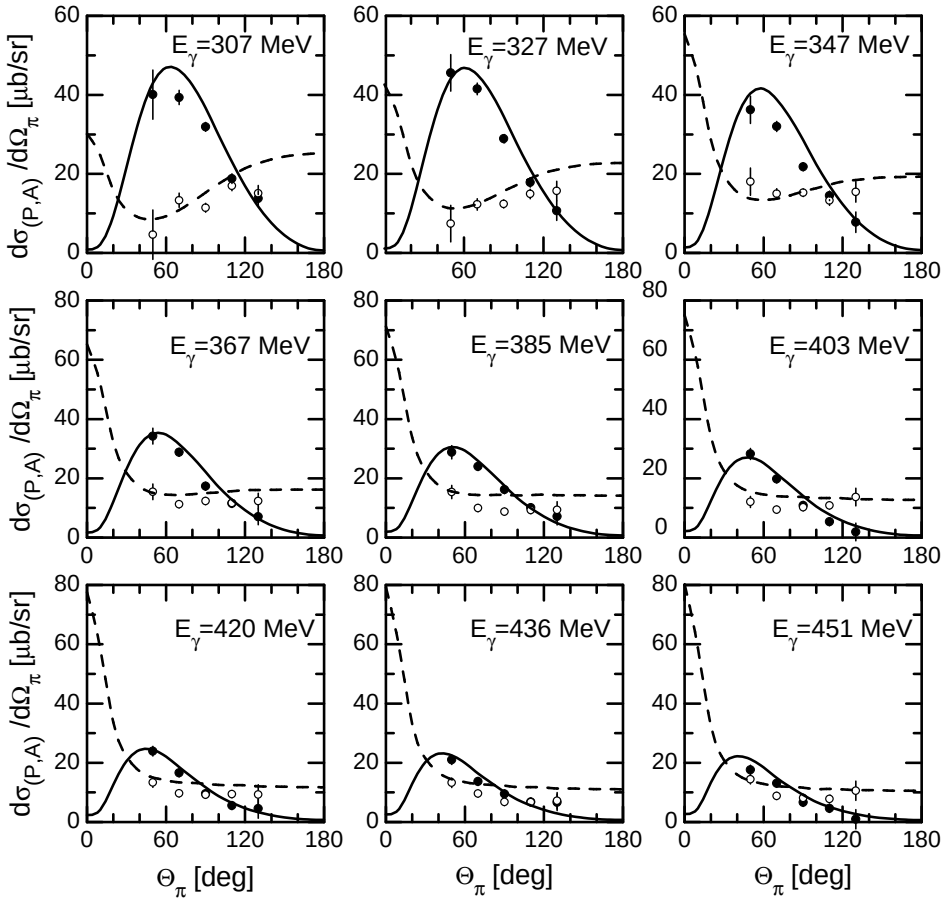

FIG. 12: Helicity-dependent differential cross sections $d\sigma_P/d\Omega_\pi$ and $d\sigma_A/d\Omega_\pi$ for the $\gamma d \to \pi^- pp$ reaction. Solid and dashed curves are our predictions for $d\sigma_P/d\Omega_\pi$ and $d\sigma_A/d\Omega_\pi$, respectively, with the amplitudes A_i and the MAID07 analysis. Data are from Ref. [11] for the parallel (•) and antiparallel (○) components. Only statistical errors are shown.

As seen in Fig. 14, our results are quite close to those obtained in Ref. [13]. Visible difference may be seen only in the neutral channel in the first resonance region.

The above disagreement also manifests itself in the value of the GDH integral, integrated up to 1.5 GeV. The upper limit of 1.5 GeV is chosen in accordance with an option from Ref. [13]. Taking into account the theoretical uncertainties, we obtain the values of 241 ± 4, -20 ± 5, and 15 ± 20 (in units of μb used also below) for the $\pi^0 np$, $\pi^- pp$, and $\pi^+ nn$ reactions, respectively, to be compared to the AFS predictions, respectively, 222, [1], -18.94, and 2.51. One can see that our value for the $\pi^0 np$ channel exceeds that of AFS by about 10%. Note here that the use of the SAID parametrization allows one to extend the upper limit in the GDH integral up to 2 GeV. With such an extension we have not found any visible changes in the result for 1.5 GeV. This means that the πNN term in the deuteron GDH integral essentially reaches convergence at these energies.

The evaluation of the GDH integral, integrated up to 350 MeV, has been performed in Ref. [15]. Results of that work with the MAID03 model for the elementary $\gamma N \to \pi N$ operator are, respectively, 123, -29, and -9 for the $\pi^0 np$, $\pi^- pp$, and $\pi^+ nn$ reactions, which are in complete agreement with our predictions of 123 ± 2, -34 ± 7, and -7 ± 10, respectively.

We have also studied the influence of the different parametrizations for the elementary $\gamma N \to \pi N$ amplitude on the value of the GDH integral, integrated to the maximum energy of 1.65 GeV. As is seen in Table I, the theoretical uncertainties in the $\pi^0 np$ reaction are quite small. They are more pronounced in the charged channels, especially in the $\pi^+ nn$ one. This considerable dependence of the results is mainly due to the multipole analyses, but the effect of

[1] In fact, this value has not been given explicitly in Ref. [13]. We have extracted it from Fig. 5 of that work making use of a digitation procedure.

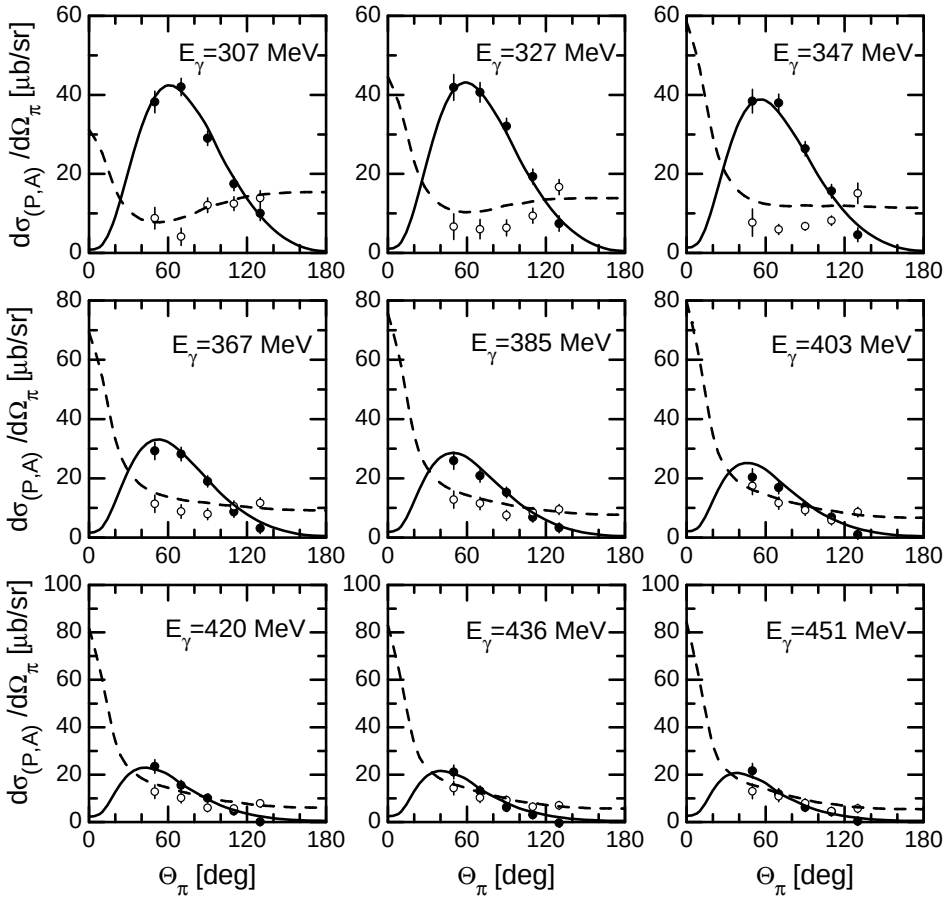

FIG. 13: Same as Fig. 12, but for the $\gamma d \to \pi^+ nn$ reaction.

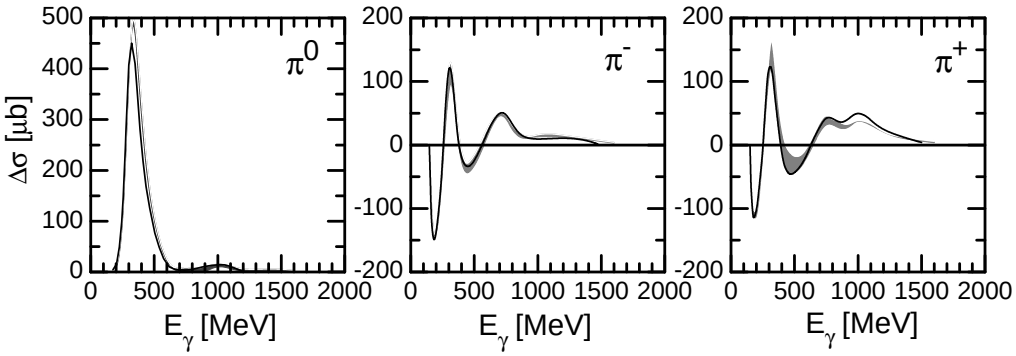

FIG. 14: Difference $\Delta\sigma$ for the separate channels of the $\gamma d \to \pi NN$ reaction. Shaded areas are our predictions with different parametrizations of the elementary $\gamma N \to \pi N$ amplitude. Curves are the AFS predictions [13].

a choice of the invariant amplitudes is also quite visible. Note that the noticeable dependence of the nucleon GDH integral evaluated with the SAID and MAID analyses was found in Refs. [18, 42]. The sensitivity of the $\gamma d \to \pi NN$ contribution to the deuteron GDH integral, integrated up to 350 MeV, to a choice of the elementary operator have been studied in Ref. [15], and considerable dependence of the results obtained with the ELA and MAID03 operators have been found.

Keeping in mind all the numbers given in Table I, we can quote our final value as 235 ± 25 μb for the contribution from the πNN channel to the GDH integral for the deuteron, integrated up to 1.65 GeV. As seen from Table I, the main part of the uncertainties stems from the $\pi^+ nn$ channel. It is worth mentioning that within the uncertainties of ± 25 μb, the AFS result of 27.31 μb [13] for the total contribution to this integral for the deuteron is compatible with

TABLE I: Sensitivity of the GDH integral (in μb), integrated up to 1.65 GeV in the $\gamma d \to \pi NN$ reaction to the parametrization of the elementary $\gamma N \to \pi N$ amplitude.

Parametrization	$\pi^0 np$	$\pi^- pp$	$\pi^+ nn$	πNN
MAID, A_i	235	–16	6	225
MAID, A'_i	238	–24	–4	210
SAID, A_i	239	–14	35	260
SAID, A'_i	241	–22	25	244

the GDH sum rule prediction of 0.65 μb.

V. CONCLUSION

The central aim of the present work is the study of the $\gamma d \to \pi NN$ reaction with the polarized photon and deuteron and its contribution to the GDH sum rule for the deuteron. To evaluate the reaction amplitude, we have used the diagrammatic model elaborated previously in Ref. [16], which takes into account diagrams corresponding to IA as well as NN and πN interactions in the final state. For the elementary operator of pion photoproduction on the nucleon, its on-shell form generated by the recent multipole analyses, SAID and MAID, has been used. Particular emphasis has been placed on the discussion of possible uncertainties introduced into the model by this operator.

Comparing our results with the recent experimental data obtained by the GDH and A2 collaborations in the energy domain from 300 to 450 MeV [9–11], we have rediscovered a known problem consisting in the sizable overestimation of the unpolarized data for the neutral channel. At the same time, the unpolarized data for the charged channels are reasonably reproduced.

We have found that the helicity-dependent differential yield difference $\Delta Y/d\Omega_p$ for the neutral channel and differential cross section difference $\Delta\sigma/d\Omega_\pi$ for the charged channels are reproduced fairly well. Also, the model provides a quite satisfactory description of the separate parallel and antiparallel yields and cross sections in all the channels.

We have also studied the uncertainties arising from the form of the elementary operator of pion production on the nucleon. Regarding the unpolarized observables, the sizable dependence has been found only for the charged channels at the lowest energy of about 300 MeV. The difference $\Delta\sigma/d\Omega_\pi$ manifests the weak sensitivity to the operator in the $\pi^- pp$ channel in the full energy domain, and the difference $\Delta Y/d\Omega_p$ in the $\pi^0 np$ channel does the same below 350 MeV. However, a large sensitivity has been found in the $\pi^+ nn$ reaction from 300 to 450 MeV at $45^\circ < \Theta_\pi < 125^\circ$.

Within our model, we have evaluated the contribution of the πNN channel to the GDH integral for the deuteron, integrated up to 1.65 GeV. In addition, the influence of the elementary operator on its value has been estimated. Our final result is 235 ± 25 μb. The uncertainty of ± 25 μb originates mainly from the $\pi^+ nn$ channel. Accepting these values as error bars for the value of 27.31 μb obtained in the AFS framework [13] for the deuteron GDH integral, one can conclude that within these error bars, the AFS result is compatible with the GDH sum rule prediction of 0.65 μb.

Further improvements of the present model are needed to resolve, at last, the problem with the strong overestimation of the unpolarized cross section in the $\pi^0 np$ channel. In particular, one should evaluate contributions of the two-loop diagrams which take into account effectively the absorption of the photoproduced π meson by the NN pair. On the experimental side, it would be very important to continue polarization measurements in the $\gamma d \to \pi NN$ channel. Specifically, data on the tensor asymmetry T_{20} together with these on the unpolarized cross section could provide the currently absent information on the $m_d = 0$ component of the reaction amplitude.

Acknowledgments

I am very grateful to A. I. Fix and P. Pedroni for valuable discussions. This work was supported by Belarusian Republican Foundation for Fundamental Research under Grant No. F09-051.

[1] S. B. Gerasimov, Yadern. Fiz. **2**, 598 (1965) [Sov. J. Nucl. Phys. **2**, 430 (1966)].
[2] S. D. Drell and A. C. Hearn, Phys. Rev. Lett. **16**, 908 (1966).
[3] K. Helbing, Progr. Part. Nucl. Phys. **57**, 405 (2006).

[4] J. Ahrens *et al.*, Phys. Rev. Lett. **87**, 022003 (2001).
[5] H. Dutz *et al.*, Phys. Rev. Lett. **91**, 192001 (2003).
[6] H. Dutz *et al.*, Phys. Rev. Lett. **93**, 032003 (2004).
[7] B. Krusche, J. Ahrens, R. Beck, M. Fuchs, S. J. Hall, F. Härter, J. D. Kellie, V. Metag, M. Röbig-Landau, and H. Ströher, Eur. Phys. J. A **6**, 309 (1999).
[8] H. Dutz *et al.*, Phys. Rev. Lett. **94**, 162001 (2005).
[9] J. Ahrens *et al.*, Phys. Rev. Lett. **97**, 202303 (2006); Phys. Rev. Lett. **98**, 039901(E) (2007).
[10] J. Ahrens *et al.*, Phys. Lett. **B672**, 328 (2009).
[11] J. Ahrens *et al.*, Eur. Phys. J. A **44**, 189 (2010).
[12] S. Hoblit *et al.*, Phys. Rev. Lett. **102**, 172002 (2009).
[13] H. Arenhövel, A. Fix, and M. Schwamb, Phys. Rev. Lett. **93**, 202301 (2004).
[14] H. Arenhövel, G. Kreß, R. Schmidt, and P. Wilhelm, Phys. Lett. **B407**, 1 (1997).
[15] E. M. Darwish, C. Fernández-Ramírez, E. Moya de Guerra, and J. M. Udías, Phys. Rev. C **76**, 044005 (2007).
[16] M. I. Levchuk, A. Yu. Loginov, A. A. Sidorov, V. N. Stibunov, and M. Schumacher, Phys. Rev. C **74**, 014004 (2006).
[17] A. Fix and H. Arenhövel, Phys. Rev. C **72**, 064005 (2005).
[18] R. A. Arndt, W. J. Briscoe, I. I. Strakovsky, and R. L. Workman, Phys. Rev. C **66**, 055213 (2002).
[19] M. Dugger *et al.*, Phys. Rev. C **76**, 025211 (2007).
[20] M. Dugger *et al.*, Phys. Rev. C **79**, 065206 (2009).
[21] D. Drechsel, O. Hanstein, S. S. Kamalov, and L. Tiator, Nucl. Phys. **A645**, 145 (1999).
[22] M. I. Levchuk, V. A. Petrun'kin, and M. Schumacher, Z. Phys. A **355**, 317 (1996).
[23] M. I. Levchuk, M. Schumacher, and F. Wissmann, Nucl. Phys. **A675**, 621 (2000).
[24] J. H. Koch and R. M. Woloshyn, Phys. Rev. C **16**, 1968 (1977).
[25] P. Bosted and J. M. Laget, Nucl. Phys. **A296**, 413 (1978).
[26] M. Benmerrouche and E. Tomusiak, Phys. Rev. C **58**, 1777 (1998).
[27] J. M. Laget, Nucl. Phys. **A296**, 388 (1978).
[28] J. M. Laget, Phys. Rep. **69**, 1 (1981).
[29] R. Machleidt, Phys. Rev. C **63**, 024001 (2001).
[30] V. G. J. Stoks, R. A. M. Klomp, C. P. F. Terheggen, and J. J. de Swart, Phys. Rev. C **49**, 2950 (1994).
[31] C. Fernández-Ramírez, E. Moya de Guerra, and J. M. Udías, Ann. Phys. (NY) **321**, 1408 (2006).
[32] D. Drechsel, S. S. Kamalov, and L. Tiator, Eur. Phys. J. A **34**, 69 (2007).
[33] G. F. Chew, M. L. Goldberger, F. E. Low, and Y. Nambu, Phys. Rev. **106**, 1345 (1957).
[34] S. Nozawa, B. Blankleider, and T.-S. H. Lee, Nucl. Phys. **A513**, 459 (1990).
[35] C. T. Hung, S. N. Yang, and T.-S. H. Lee, J. Phys. G **20**, 1531 (1994).
[36] C. T. Hung, S. N. Yang, and T.-S. H. Lee, Phys. Rev. C **64**, 034309 (2001).
[37] M. Schwamb, Phys. Rep. **485**, 109 (2010).
[38] U. Siodlaczek *et al.*, Eur. Phys. J. A **10**, 365 (2001).
[39] E. M. Darwish, H. Arenhövel, and M. Schwamb, Eur. Phys. J. A **16**, 111 (2003).
[40] P. Benz *et al.*, Nucl. Phys. **B65**, 158 (1973).
[41] H. Arenhövel and A. Fix, Phys. Rev. C **72**, 064004 (2005).
[42] R. A. Arndt, W. J. Briscoe, I. I. Strakovsky, and R. L. Workman, Phys. Rev. C **72**, 058203 (2005).